HYBRID LAMINAR FLOW NACELLE DESIGN

J.L. Lecordix, Snecma, Moissy-Cramayel - France
A. Mullender, Rolls-Royce, Derby - United Kingdom
E. Lecossais, Hispano-Suiza, Le Havre - France
J.L. Godard, ONERA, Chatillon - France
M. Hepperle, DLR, Braunschweig - Germany

Abstract

One of the effects of the increase in bypass ratio is that turbojet nacelles contribute increasingly towards the total drag of the aircraft. Therefore installing systems on nacelles to maintain laminar flow over a large portion of the nacelle surface can reduce the engine specific fuel consumption by over 2%.
To meet this objective, hybrid laminar flow (HLF) technology takes advantages from both natural laminar flow (NLF) technology and laminar flow control technology (LFC). Consequently, while producing a very large increase in laminar flow over the design point it enables laminar flow to be maintained over a larger extent of the flight envelope and ensures low-speed performance as good as with conventional nacelles.

In pursuit of this objective, Rolls-Royce, Snecma, Hispano-Suiza, ONERA and DLR decided to collaborate to study the design of an HLF nacelle. It was within the European programmes ELFIN II and LARA, backed by the European Community, that the five partners developed an HLF nacelle design corresponding to the characteristics of a large modern aircraft turbojet.
Two test campaigns were carried out: one at low speed with a small model and one at high speed with a large model featuring a boundary layer suction system. These tests fully performed the required low-speed performance levels and showed a very large extent of the laminar boundary layer up to very high Mach numbers.

This paper describes the work carried out during these two programmes and presents a summary analysis of the results obtained from the two wind tunnel test campaigns.

Introduction

One of the main task of aeronautical design engineers is to reduce the drag of the aircraft they design. In the field of commercial aircraft, a direct effect of reducing drag is a reduction in specific fuel consumption, leading to savings not only in the cost of fuel consumed but also, with a reliable device, in the weight of fuel carried, permitting an increase in either the payload or the operating range of the aircraft. Moreover, indirect effects of the reduction in specific fuel consumption include a reduction in toxic emissions (NO_2, CO, etc.) and a reduction in power and therefore the size and cost of the engine.

One of the most important components in the drag of a subsonic aircraft is friction drag. Early studies revealed the highly substantial gains that could be obtained in this field through adequate control of the nature of the boundary layer. Thus began the research into laminar flow which occupied many specialists before, during and after the 2nd World War. These studies first concentrated on the natural control of the boundary layer by designing profiles that enabled the flow to be kept in acceleration for as far as possible. Application of this technology to aircraft wings reached its limits with the advent of swept wings, and the failure to solve the problems of contamination and compliance with low-speed performance requirements.

To overcome this, many researchers envisaged introducing a wall suction system to maintain laminar flow. In the early 1960's, the NASA flew a WB66 equipped with an entirely porous wing [1]. In certain flight conditions the flow remained laminar over 80% of the wetted surface of the wing. More recently, in the subsonic civil transport aircraft field, Boeing flew a B757 equipped with a laminar wing glove and demonstrated a potential gain induced by this technology [2]. Similar studies were initiated by the European aircraft manufacturers during the 1980's, some of which were grouped together in the European programmes ELFIN I and II [3].

For many years studies in laminar flow technology concentrated on aircraft wings. However, since the beginning of the 1980's, several teams have studied the problems of laminar flow turbojet nacelles.

General Electric, followed by Pratt & Whitney and NASA started by examining natural laminar flow nacelles [4]. Although this technology is attractive for the nominal flight points it becomes ineffective at high Mach numbers and does not sustain the required low-speed performance levels. Subsequent studies concentrated on the combination of the natural and suction technologies in a single concept which led to the technology of hybrid laminar flow nacelles (HLF). Among the recent studies conducted along these lines it is worth mentioning; the flight tests performed by GE/ROHR/NASA on a CF6-50A2 engine nacelle installed on an Airbus A300 where the laminar flow was maintained up to the nacelle maximum cross-section[5]. Rolls-Royce, MTU and the DLR for their part carried out in-flight tests of NLF and then HLF nacelles on a Rolls-Royce/Snecma M45H engine installed on VFW614 of the DLR [6]. During the 93 hours flown, laminar flow was maintained over 60% of the chord.

Convinced of the potential of the application of HLF technology to turbojet nacelles, Rolls-Royce as subtask manager, Snecma, Hispano-Suiza, ONERA and DLR embarked upon an ambitious research and development programme into this technology. In the context of the research programmes backed by the European Community, several manufacturers, research institutes and universities collaborates under the supervision of Daimler-Benz Aerospace Airbus in the ELFIN II and LARA programmes for research into laminar flows on subsonic civil aircraft. Within the framework of these programmes, RR, Snecma, HS, ONERA and DLR have studied, in specific tasks, the design definition of a HLF nacelle for a modern turbojet combining the following severe constraints: large-size engine (110 inches fan diameter with a high bypass ratio leading to a high in-flight chord Reynolds number (33 million), high cruising speed (M = 0.83), maintaining laminar flow over a large portion of the flight envelope characterised by a variation of the flight Mach number from 0.7 to 0.85, the thrust from 75% to 100% of the max. cruise requirement and the angle of attack from 2° to 6°.
Furthermore, the nacelle was required to sustain low-speed flight performance levels that were as good as the most exacting demanded of modern aircraft.

As part of the ELFIN II subtask 1.2, the five partners first defined the aerodynamic design of the nacelle, then they designed and built a model which was tested in ONERA's transonic tunnel S1. At the same time, as part of the LARA programme, nacelle performance at low speed was analysed and verified in ONERA's wind tunnel F1. A preliminary analysis of the installation effects was also performed.

Design

Optimisation of Mach number distribution

The first stage in the design of a HLF nacelle involves finding the optimum Mach number distribution. This study was carried out by Rolls-Royce using the JA61 redesign code solving potential equations and the VP97 boundary layer code based on an integral method and used to determine the suction flow rate required to maintain a laminar boundary layer flow[7], [8]. This study was carried out on axisymmetric geometries

Figure 1 illustrates the shape of three of the analysed Mach number distributions. These Mach distributions include a deceleration between 10% and 20% of the chord which requires boundary layer suction to maintain laminar flow. At the end of this region, the Mach number is low which permits an acceleration from 20% to 60% of the chord sufficient to maintain laminar flow while keeping the Mach number at the max. cross section below the value which could create a strong shock.

The optimum choice took into account the maximum extension of the laminar zone, the required suction flow rate and the leading edge curvature. We were also concerned about moving the suction zone sufficiently far from the leading edge to be able to integrate a de-icing system. In accordance with all these criteria, a profile was chosen as the starting point for the three-dimensional design study.

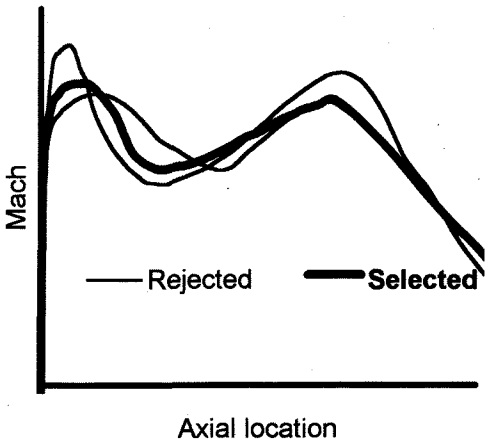

FIGURE 1 - Mach Distribution Selection

3D Iterations

The next stage concentrated on finding nacelle shapes that were suitable for the chosen engine, while respecting the selected form of Mach number distribution at the cruise design point, and which were capable of sustaining the required low-speed performance levels. The partners examined four designs during this stage. Snecma designed the nacelles from its redesign code solving the full potential equations and calculated performances at low speeds using a 3D code called SESAME which solves the Euler equations on structured multiblock meshes [9], [10]. These two codes were developed at ONERA. Rolls-Royce calculated the performance at high speed in off-design conditions (Spillage, Divergence, AOA variation) using the JA61 code, and ONERA studied the suction levels required to maintain laminar flow at the cruise point.

The suction specifications could be prescribed after a complete boundary layer and transition prediction investigation. The boundary layer was computed with a code developed at ONERA/CERT, solving the equations with a finite volume method using a three-dimensional grid of the viscous flow, and simulating the boundary layer suction. Inside this code the transition location can be determined with transition criteria developed at ONERA/CERT: the so-called database method based on the theory of laminar instability is used for longitudinal instabilities and a criterion deduced from experiments is used for cross-flow instabilities [11], [12]. In addition for a limited number of cases, complete stability computations were performed and confirmed the results given by the criteria.

During these 4 iterations, keeping the Mach number distributions axisymmetric around the nacelle, in order to avoid causing transverse instabilities that favour boundary layer transition, was a constant concern. The optimisation of these different projects concerned not only the shapes of the external profiles but also the adaptation of the inlet geometries, particularly the droop angle and the internal contraction ratios.

During the design phase of the three-dimensional nacelle only the cruise conditions were considered for the optimisation of the suction region (flight Mach number 0.83, Angle of attack 4 degrees, nominal engine massflow, Reynolds number 33 million). For each iteration of nacelle shape, several extensions of the suction region were considered with a variation of suction velocity, and an optimal suction extent with an optimal suction velocity were determined, corresponding to the lowest massflow sucked in the boundary layer leading to an extended laminarity.

Figures 2a and 2b show the change in cruise performance for these four projects, in terms of laminarity percentage and required suction flow rate. The second project had to be eliminated because low-speed performance was inadequate (external boundary layer separation with engine at idle). The other three projects were all acceptable in terms of performance in off-design conditions. Finally, the last project was chosen because it offered the best compromise between the extension of the laminar zone and the suction massflow. Figure 3 shows a side view of the nacelle with the position of the suction zone and the transition location. This is caused by a laminar separation generating a separation bubble, after which the flow reattaches but with a fully turbulent boundary layer. This location corresponds to a Reynolds number equal to 23million.

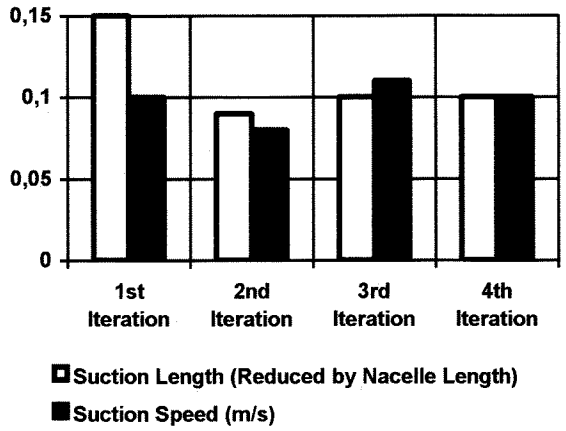

FIGURE 2a - Suction Characteristics

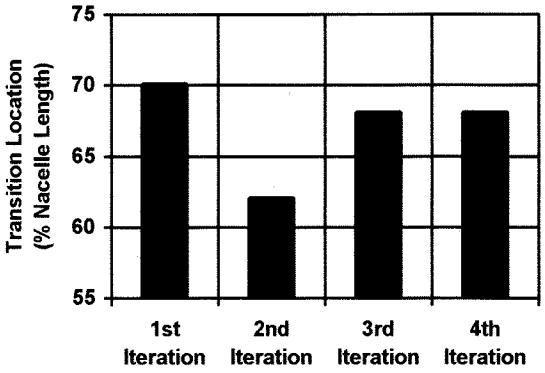

FIGURE 2b - Laminar Flow Extension

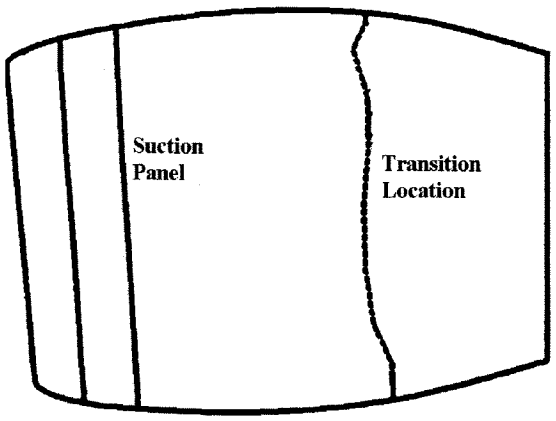

FIGURE 3 - Transition Location

For the final project a 3D Euler calculation was performed by Snecma taking into account the fan nozzle exhaust flow. Although introducing this parameter slightly modified the Mach number distributions from the maximum cross-section onwards, it did not contradict the overall results, as transition occurred at the same place and for the same reasons.

Design of the axisymmetric nacelle

A simplified form of the preceding design was taken to carry out wind tunnel tests with boundary layer suction. For reasons of manufacturing simplicity, the wind tunnel model was axisymmetric and its diameter in the hilite plane was limited to 1.20 meter.
The appropriate shape of the axisymmetric nacelle was obtained from the lower line of the 3D nacelle. In the wind tunnel set-up, the nacelle is supported by a downstream cylindrical duct. The design of the blending radius between the nacelle trailing edge and this duct was optimised in order to produce a Mach number distribution very similar to those obtained in the 3D project, as can be seen in figure 4.

The aerodynamic conditions for the tests at the ONERA S1MA wind tunnel are slightly different from the flight conditions : model scale 1/2.5 and Reynolds number 24 million (2/3rd of the flight Reynolds number). Furthermore, as the extended laminarity was desired not only for the cruise conditions but for an envelope of aerodynamic conditions during the tests, in addition to the cruise conditions, three other ones, representative of the extreme nacelle operating conditions, were defined :

- 75% of net thrust at M = 0.83, $\Delta\alpha = +2°$
- 75% of net thrust at M = 0.85, $\Delta\alpha = 0°$
- 100% of net thrust at M = 0.83, $\Delta\alpha = +2°$

The first point gives the most sudden recompression in the suction zone where extended laminarity is required. As regards the 2nd point, it provides a check that the overspeed levels reached in the region of the maximum cross-section do not cause the separation of the flow.

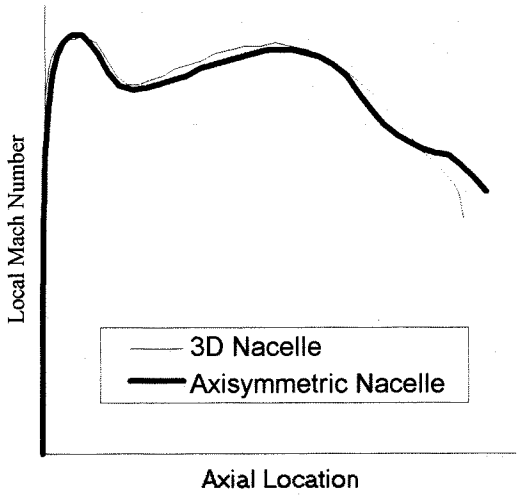

FIGURE 4 - 3D and Axisymmetric Nacelles
Mach Distribution Comparison

Due to these new requirements, it was necessary to perform a new suction optimisation. The same codes were used as during the three-dimensional nacelle design phase. As a conclusion it came out that it was necessary to change the suction region which extended from 9% to 23 % of the chord for the new design. The suction speed necessary to achieve an extended laminarity varied from 0.10 m/s for the cruise condition to 0.25 m/s for the most critical case (75% net thrust, AOA 2 degrees).

Figure 5 presents the evolution of the amplification factor N, representative of the intensity of longitudinal perturbations. Both 3D and axisymmetric nacelle calculations were done for cruise conditions but with different Reynolds numbers and suction extent. The evolution is slightly different but the transition occurs downstream in the two cases, and is due to a laminar separation at the beginning of the downstream deceleration..

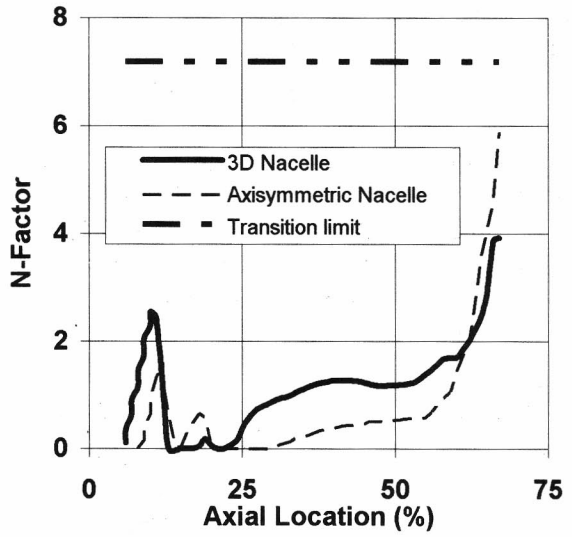

FIGURE 5 - N-Factor Evolutions

A final numerical study of the axisymmetric configuration was undertaken by Snecma. In order to check that the wind tunnel installation did not excessively disturb the flow around the nacelle, a calculation that took into account the nacelle, its pylon and the wind tunnel walls was performed. This model was not perfect however, because the wind tunnel walls feature slots to prevent blockage, and these slots were not modelled. Figure 6a shows the calculated Mach number field and figure 6b shows a comparison of Mach number distributions in isolated and installed conditions. In spite of the fact that the slots were not modelled, this result confirms that installation in the wind tunnel section did not seriously disturb the behaviour of the flow, which kept zones and intensities of recompression or acceleration very close to those desired.

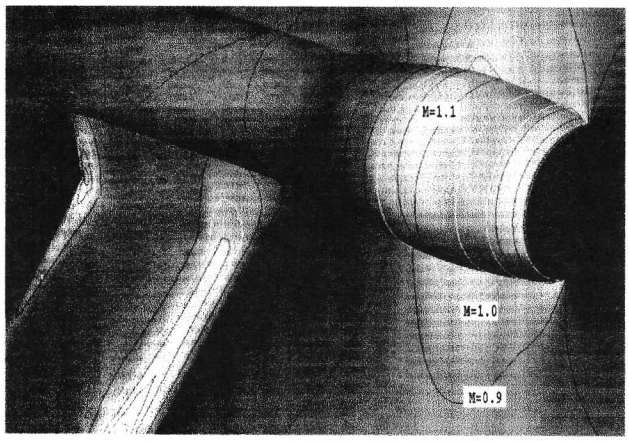

FIGURE 6a - Wind Tunnel Configuration - CFD Calculation at Cruise Condition - Mach Contours

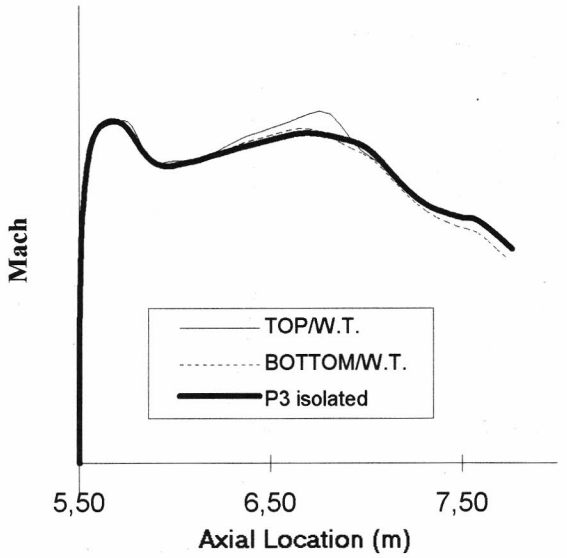

FIGURE 6b - Wind Tunnel Installation Effect - Mach distributions.

Prediction of Installation Effects

When a nacelle is installed close to the wing of an aircraft, it operates under the influence of pylon, wing, and fuselage. The installation effects on a HLF nacelle may be larger than on a conventional nacelle, because the position of the maximum thickness of the HLF nacelle is shifted downstream.

For the numerical evaluation of the installation effects, DLRs generic transport configuration ALVAST was selected. Its planform is similar to an Airbus A320 aircraft and its design Mach number is M_{Design}=0.785, which is lower than the nacelle design Mach number $M_{Nacelle}$=0.83. To reduce the shock strength on the upper wing surface, the sweep angle of the wing was increased to 32°; the lower surface exhibits no shock.

The nacelle position was chosen close to the standard CFM-56 engine installation as shown in figure 7. The numerical results were obtained using the DLR solver CEVCATS , which solved the Euler equations on a structured grid of approximately 750000 cells [13].

In figures 8a, 8b and 8c, the results of the installed nacelle analysis are compared to results obtained for the isolated nacelle. As expected, the strongest influence can be seen in the neighbourhood of the pylon (figure 8a), most pronounced at the inboard position (θ=340°). Here the installation causes a

complete loss of the favourable pressure gradient, so that no laminar flow can be expected behind the suction region. The rear part of the corresponding outboard section at θ=20° shows a pressure distribution similar to the isolated nacelle one, but with a reduced gradient between suction region and the location of the maximum thickness. Laminar flow is rather unlikely to be achieved in this region of the nacelle.

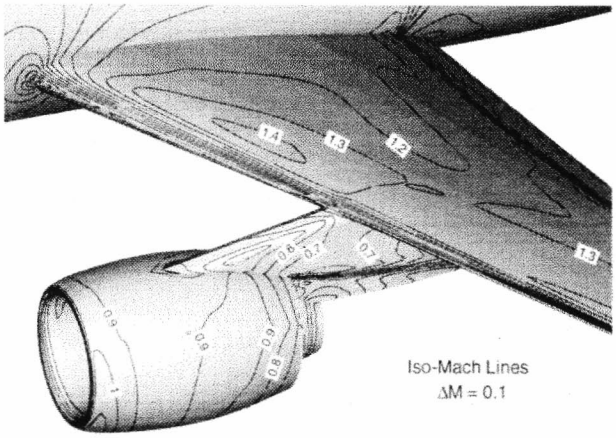

FIGURE 7 - 3D Nacelle Installation
Mach Contours in Cruise Condition

A horizontal cut through the nacelle (figure 8b) still shows a rather strong reduction of the pressure gradient on the inboard side (θ=270°), whereas laminar flow might be possible on the outboard side of the nacelle (θ=90°). A further reduction of the installation effects is visible on the lower side of the nacelle (figure 8c) at θ=180°, where the pressure gradient is reduced, but still favourable.

The results of the installed nacelle analysis have shown, that it is extremely important to take into account the installation effects during the design of a HLF nacelle. We did not take into account this effect for the design of the 3D nacelle. In deed the ELFIN II program was deliberately dedicated to the isolated nacelle design and test. Installation effects will be integrated in a future program.

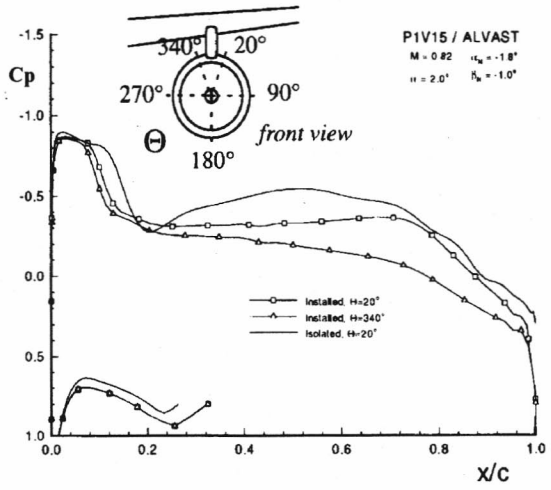

FIGURE 8a - Pressure distributions on the top sections of the nacelle

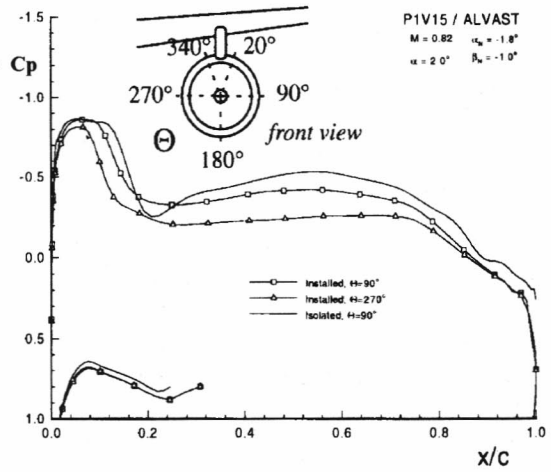

FIGURE 8b - Pressure distributions on the side sections of the nacelle

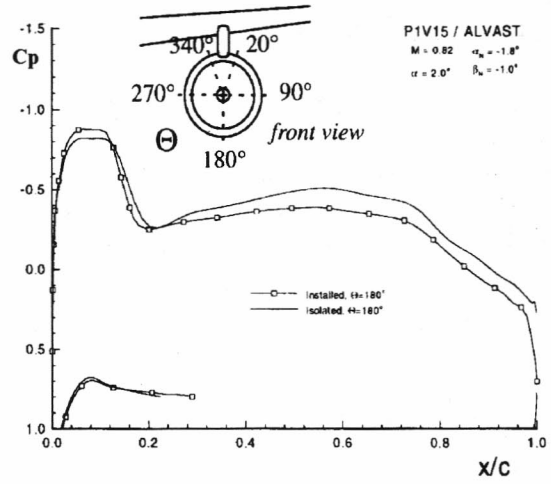

FIGURE 8c - Pressure distributions on the bottom section of the nacelle

Low Speed Wind Tunnel Test

Low-Speed Wind Tunnel Model

The wind tunnel model for the low-speed, off-design tests was designed and manufactured by DLR. The model corresponded to the 3D nacelle at scale 1/8.33, which gave a length of 0.65 m and a hilite diameter of 0.36 m (figure 9). Because the model was specifically designed for the evaluation of the off-design behaviour at large angles of attack and yaw, no boundary layer suction system was necessary.

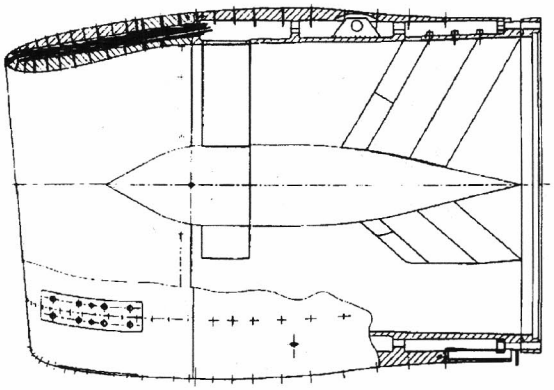

FIGURE 9 - Low Speed Test Model

This model was equipped with 150 total pressure taps on rakes located at the engine fan face and 260 static pressure taps on the surface.

Low-speed test facility

The low-speed tests were carried out in ONERA's F1 wind tunnel at the Le Fauga-Mauzac centre. This wind tunnel has a 4.5 by 3.5 metre test section. The maximum speed in the test section is 120 m/s. This wind tunnel can be pressurised, and the total pressure can reach 4 bars.

These characteristics mean that the wind tunnel is well suited to the analysis of inlet performance at low speeds, guaranteeing Reynolds numbers close to those reached in flight. As the model support can be tilted up to 35°, it can be installed in the vertical or horizontal position in order to study flight conditions in crosswind or headwind conditions. Figure 10 shows a photograph of the model installed in the headwind configuration.

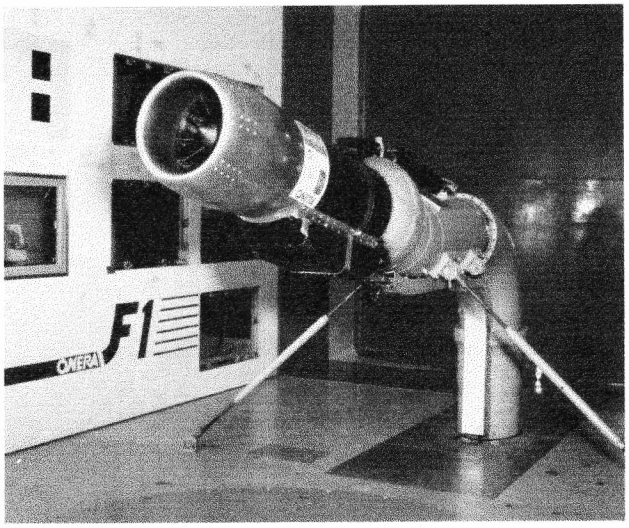

FIGURE 10 - Wind Tunnel Test Set-up

Crosswind test results

The crosswind tests were performed by making slow engine airflow sweeps at a constant crosswind speed. Measuring the total pressure field in the engine intake plane gives the level of distortion generated by the inlet. In figure 11 the distortion levels expressed by the circumferential distortion coefficient (IDC) are presented; two crosswind speed measurements are indicated. By setting a permissible maximum limit of 10%, this diagram shows that the inlet provides acceptable distortion levels up to a crosswind component of 35 Kt, in compliance with the certification specifications.

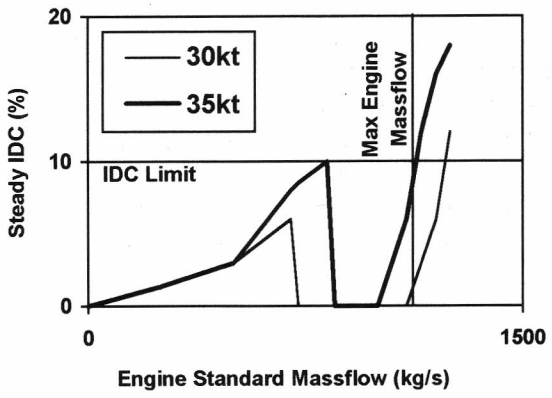

FIGURE 11 - Crosswind Performances

Civil aircraft often apply a gradual acceleration procedure, called Rolling Take-Off (RTO), during

crosswind conditions, thereby reducing the level of distortion ahead of the engine. Consequently, the engine does not reach maximum power until the aircraft reaches speed (usually 60 kts). Wind tunnel tests have been performed for this operating condition. The results are summarised in figure 12. It shows that by adopting a rolling take-off procedure, the inlet is capable of operating at up 1250 kg/s, that is to say 100 kg/s more than the initial target, without delivering airflow marred by an excessively high distortion level for the engine.

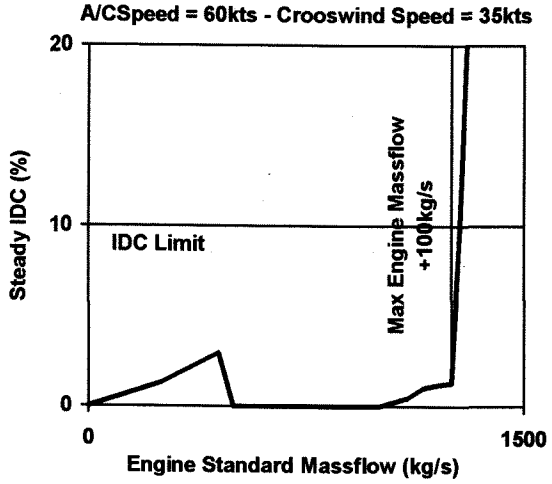

FIGURE 12 - Crosswind Performance with RTO Procedure

Headwind results

Another important performance parameter for an inlet is its ability to maintain high angles of attack at low speeds, without delivering to the engine an airflow with an excessive level of distortion. The wind tunnel experimental validation procedure is the same as for crosswind conditions. Slow changes in engine airflow are made while total pressure distortion is measured by the rake sensors. These measurements are nevertheless supplemented by slow sweeps in angle of attack with the airflow at its maximum required value. The distortion levels measured during these variations provide an indication of the maximum angles of attack accepted by the inlet as a function of flight Mach number.

Figure 13 shows the measured angles of attack of internal separation as a function of Mach number, compared with the targets and numerical predictions. The tests confirmed compliance with targets, and even showed a 2° safety margin. This result is very close to the initial numerical predictions done by Snecma, with a difference of less than 1° in all cases.

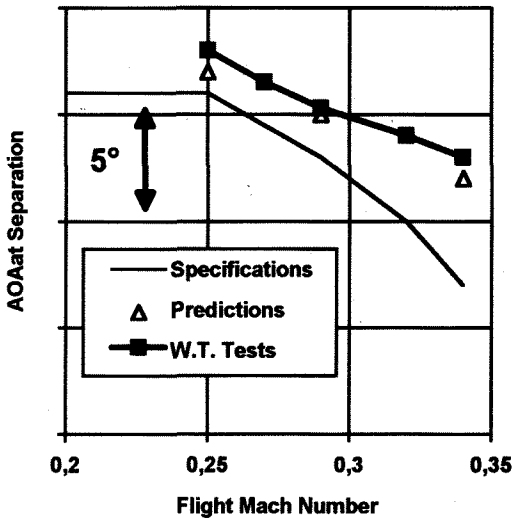

FIGURE 13 - Headwind Performance

The margin between the target angle of attack and the experimental results can be advantageous to the engine in terms of increased maximum airflow and hence increased take-off thrust. The synthesis of the measurements made during flow variations at target angles of attack shows that the inlet remains compatible with the level of distortion demanded by the engine up to a massflow rate of 1200 kg/s, giving a 50 kg/s margin over the initial specifications.

External separation

The last important performance-related parameter required for an inlet under low speed flight conditions is its ability to accept high angles of attack with a failed or idling engine. Under such flight conditions, there must be no separation of the airflow around the nacelle as this could reduce wing lift, and affect aircraft control and stability.

These performance parameters are tested in the wind tunnel by making slow angle of attack sweeps at flight idle or windmilling airflow. As this flight condition is highly sensitive to the Reynolds number, it is tested under various conditions which can be easily reproduced in the pressurised wind tunnel. Figures 14a and 14b show the external separation angles of attack measured as a function of Mach number with the engine idling and windmilling. They are compared with the initial targets and the predictions. In this case, the experimental results are about 1° below the predictions. However, they still remain better than the targets, and therefore substantiate the design as regards external separation behaviour.

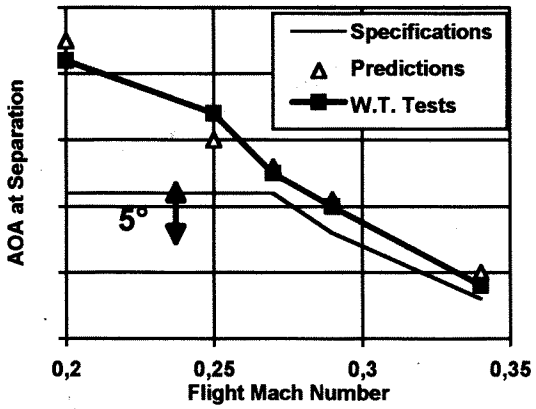

FIGURE 14a - Windmilling Performance

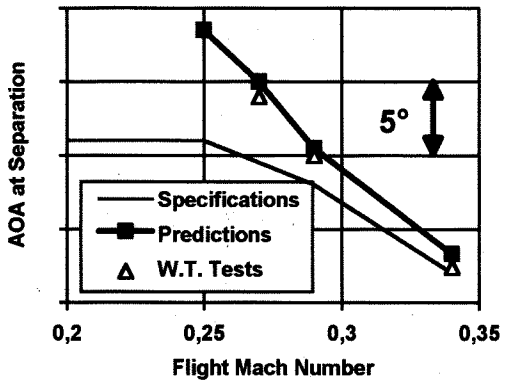

FIGURE 14b - Flight Idle Performance

These results were obtained at the highest Reynolds number attained in the wind tunnel without extrapolating the test results up to the flight Reynolds number. Such a correction indicates a margin exceeding 1° at flight Mach numbers of less than M=0.3, but becoming very low at M=0.34, the most critical flight point. The inlet therefore just meets the initial external separation objectives without providing an additional margin. This means that it is well suited to the HLF nacelle concept.

Conclusions Regarding Low Speed Performance

The inlet designed for the HLF nacelle meets all the required low-speed flight specifications. More specifically, it meets the external separation requirements, which are determined by the curvature radius of the leading edge of the upper line. This is of prime importance, because these requirements are difficult to achieve on hybrid or natural laminar flow nacelles. Moreover, distortion performance levels exceed the objectives, giving a 50 kg/s gain in airflow. In our project, this could be used to reduce the inlet throat and hilite areas by more than 2%, giving an increased massflow ratio coefficient in cruise condition which is favourable to the maintenance of laminar flow.

High Speed Wind Tunnel Tests

High Speed Wind Tunnel Model

- Suction System

The extent of the suction was defined during the design phase as from 9% to 23% of the chord. It was decided to implement this suction system over three quarters of the nacelle circumference keeping one quarter as reference.

ONERA made the proposal for the mechanical arrangement of this suction system (figure 15). This system is composed of a perforated suction panel placed at the surface of the nacelle and different suction compartment inside the nacelle. Each compartment is divided into chambers separated by thin walls supporting the suction panel. The pressure inside each compartment can be prescribed with a suction system provided by the test centre and connected to the compartments by pipes. The pressure inside each compartment must be lower than the pressure outside the nacelle to enable a boundary layer suction.

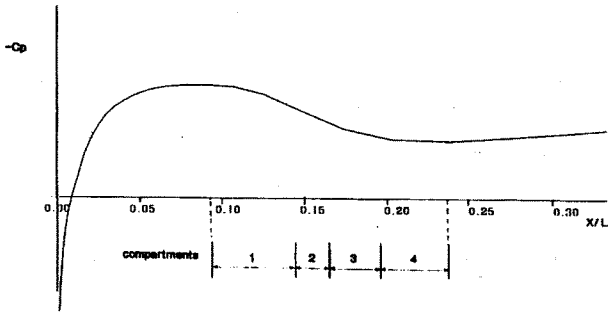

FIGURE 15 - Suction System Layout

The distribution of the different suction compartments was defined, as well as the characteristics of the suction panel: a panel with 60. micron holes with a porosity of 0.39% was proposed, leading to an estimated pressure loss characteristic versus the suction velocity. The suction to prescribe inside the compartments was estimated. All these characteristics are the result of a

compromise between the different constraints coming from the range of suction velocities to be obtained during the tests. The maximum velocity is limited by the minimum pressure that can be prescribed in the compartments, and the minimum suction is limited by the risk of outflow, and all this depends on the external flow. Finally, we selected a design with 12 compartments, with a 4 (axial) x 3 (circumferential) distribution.

Several inspections were performed on this suction system, at different stages of the manufacture. In addition to leakage tests, pressure loss characteristics of each suction panel for different suction velocities were determined. These measurements were both local and for each complete compartment. The final inspection at the end of the nacelle manufacture gave an average pressure loss for each compartment approximately 80% higher than the specifications. This difference had no consequence on test programme achievement but illustrates the difficulties in predicting the characteristics of a suction panel. These differences can come from the manufacture process of the suction system, but also from limited experience concerning the use of stainless steel.

- Model Manufacture

To obtain a realistic simulation of the boundary layer behaviour under flight conditions in a wind tunnel environment, it is important to have a large scale model to achieve a representative Reynolds number. Due to manufacture constraints and the size of the test section , a model of scale 1/2.5 was realised, with an hilite diameter of 1.2 meter and a reference length of 2.050 meters leading to a Reynolds number of 24. million at cruise conditions: two third of the Reynolds number for the real engine in flight.

The model is divided in different sub-structures; the main ones are the inlet including the suction compartments and the leading edge, the composite panel corresponding to the external surface and the internal sub-structure which supports the previous sub-structures, the suction tubes and the plug. The suction panel was manufactured from stainless steel to ease the fabrication process; the same material was selected for the leading edge to avoid thermal expansion problems. A carbon fibre aluminium core sandwich duct has been designed for the after body of the nacelle to allow transition viewing by infra-red cameras and also to eliminate aluminium of the external nacelle surface with its high coefficient of expansion. During tests the wind tunnel temperature increased to approximately 50°C and therefore the model had to withstand it without adversely affecting aerolines or aerosmoothness. The support tube was manufactured from 20 mm thick sheet aluminium, the plug and pivoting pylon fairing were also manufactured in aluminium. The plug was 2 meters long and included an actuator in order to control the massflow in the inlet during the tests.

To achieve large extents of laminar flow, very good surface quality was required. Both waviness and steps and gaps tolerances should be far below those required for conventional nacelles as illustrated in table 1 and 2 and figures 16a and 16b.

Nacelle	ELFIN II Nacelle	Conventional A/C Nacelle
Deviation from Loft contour	±0.5 mm (under loads)	±1.6 mm (free)
Max. wave amplitude	0.03 inch'	0.09 inch
Max. wave ratio D/L	0.004	0.005
Max. slope D/X	0.016	0.01

Table 1 - Waviness requirements

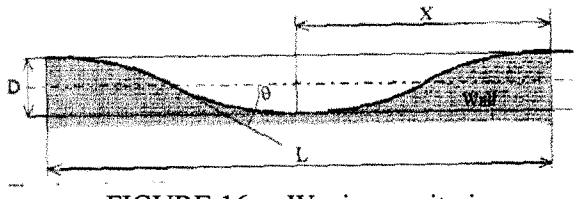

FIGURE 16a - Waviness criteria

Nacelle	ELFIN II Nacelle	Conventional A/C Nacelle
Max. forward facing step	0.1 mm	0.4 mm (class I)
Max. backward facing step	0.03 mm	0.4 mm (class I)
Maximum gap	0.1 mm	0.03 inch

Table 2 - Steps and gaps requirements

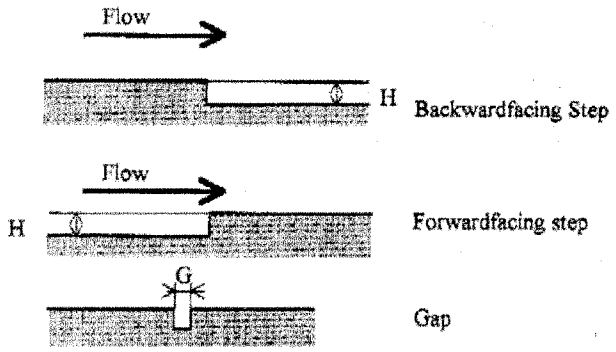

FIGURE 16b - Steps and Gaps Criteria

- Instrumentation

The instrumentation of the HLF wind tunnel model (figure17) was defined to have a good description of the flow around the nacelle and of the boundary layer behaviour, without disturbing the sensitive boundary layer. Thus the number of sensors on the model surface was kept at a minimum and their arrangement was carefully chosen to minimise the risk of provoking premature transition. The pressure measurement equipment consisted of static surface pressure taps, boundary layer and large flow field rakes. The boundary layer state was determined by hot film sensors, surface temperature sensors, infra red cameras, and small boundary layer rakes. One of the rakes was installed on the quarter of the nacelle which was not equipped with suction panels, to measure reference values in turbulent flow. The external drag calculation took into account the viscous drag and the wave drag; these drags were calculated for each rake by integrating the total pressure losses as usually done in the S1 wind tunnel, taking the hilite area as reference.

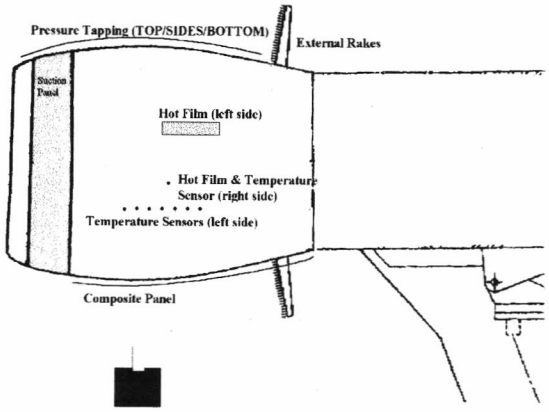

FIGURE 17 - Sketch of the Instrumentation

In general, the instrumentation worked very well, and had no detrimental effect on the development of laminar flow. Only the temperature sensors, which had been successfully used in a similar arrangement during previous HLF nacelle flight tests, gave no helpful information on the boundary layer state [6]. This might be caused by the fact, that they had not been installed perfectly, and by the much higher temperature level in the wind tunnel.

Due to the homogenous honeycomb structure of the nacelle, the infra red images were of high quality, only slightly influenced by reflections from the wind tunnel walls (windows and slots). In the pictures include in this paper, laminar flow appears as darker regions.

Wind Tunnel Set-up

The tests in cruise conditions at high subsonic speed were performed in the ONERA-S1MA wind tunnel. Its test section is roughly circular, 8. meters in diameter.

The set-up is presented in figure 18. The nacelle itself is prolonged by a cylindrical tube and the model is supported by a pylon fixed on this rear tube. With this set-up the nacelle is close to the wind tunnel axis. The attachment between the pylon and the model allows variations in the angle of attack.

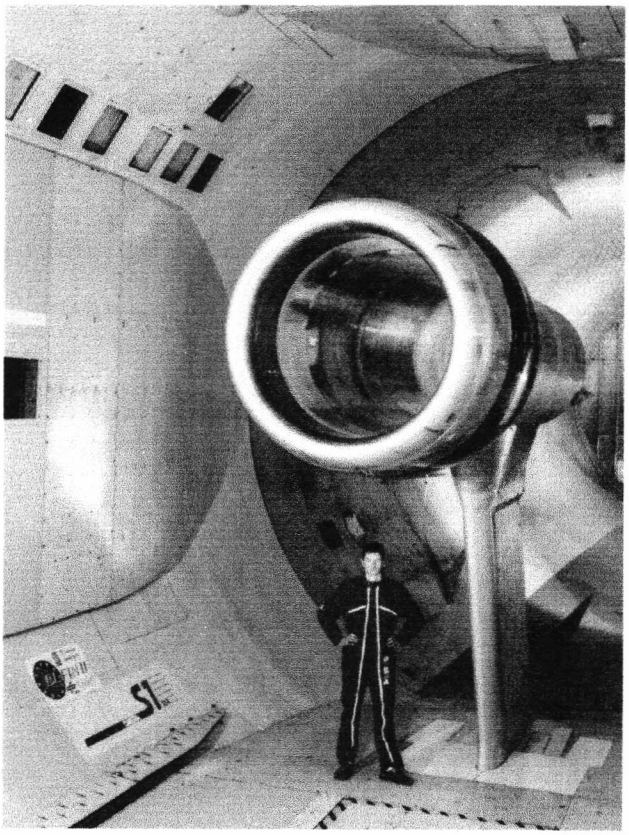

FIGURE 18 - High Speed Wind Tunnel Set-up

Test results

Analysing the test campaign for a hybrid laminar flow nacelle is a long process. Due to short time since completing the tests, only preliminary results are presented in this paper, based in particular on the analysis of infrared images and boundary layer thickness measurements using external rakes.

The test campaign lasted five days, with the first three days being devoted to the study of the nacelle behaviour with an angle of attack of zero degree and the last two to behaviour with an angle of attack of 2°. Throughout the campaign the joint between the microperforated plate and the leading edge or the

carbon skin was refinished to avoid steps and gaps and waviness as much as possible.
Performance levels improved continuously during the test due firstly to the improvement of the joints and secondly to a better monitoring of the suction distributions and temperature conditions.

- Results at 0° angle of attack

With a zero degree angle of attack the most extensive laminar flow was obtained at M = 0.78. The infrared image (figure 19) shows a large laminar zone on the upper left-hand quarter of the nacelle, with a transition point at between 50 and 60% of the nacelle length. Turbulent wedges are clearly visible, indicating that transition could be caused by insufficient surface quality. Extension of the laminar region is confirmed by the hot film signal, which shows an unstable dynamic signal oscillating between laminar and turbulent flow. The most remote the station of the sensor of the hot film the greater the turbulent flow signal, with laminar flow disappearing completely beyond 70% of the chord (figure 20). On the infrared image a large section remains completely turbulent. This corresponds in fact to the junction between two suction chambers where suctions can not be applied and laminar flow controlled.
These results can be synthesised by the display of drag levels measured by the rake placed downstream of this zone (figure 21).

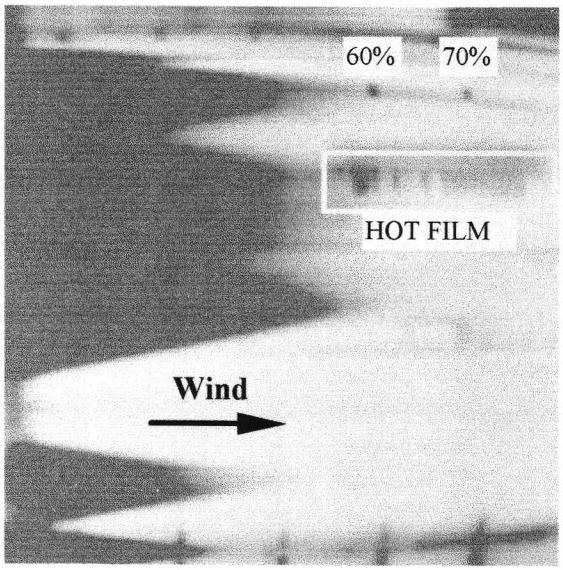

FIGURE 19 - Infra-red Picture - M=0.78 - No AOA

The upper and lower boundaries of the cluster of points show drag changes as a function of the wind tunnel Mach number, these curves being obtained without suction and with optimum suction respectively. In this analysis, optimum suction is only defined on the drag reduction without taking into account penalties coming from the power required by the suction system. The upper boundary indicates that turbulent drag is virtually constant with the external Mach number up to M = 0.84. For the laminar flow boundary, the effect of external Mach number is very noticeable, with a reduction in drag up to M = 0.78, whereas beyond this value it was impossible to achieve laminar flow. The reduction in external drag between M = 0.7 and 0.78 is confirmed by the infrared displays recorded during the same test run (figures 22a and 22b) and which clearly indicate an increase of nearly 10% in the extension of the laminar zone upstream of the rake, between M = 0.7 and M = 0.78. The area upstream of the rake (θ = 45°) can be easily identified with the hot film position (θ = 40°).

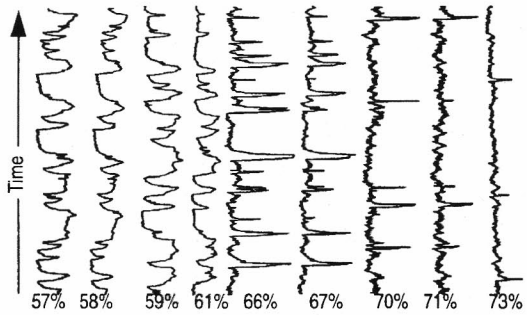

FIGURE 20 - Laminar/Turbulent Detection by Hot Film - The signal covers a range in time of 160ms. Intermittent signals at 57% indicate transition.

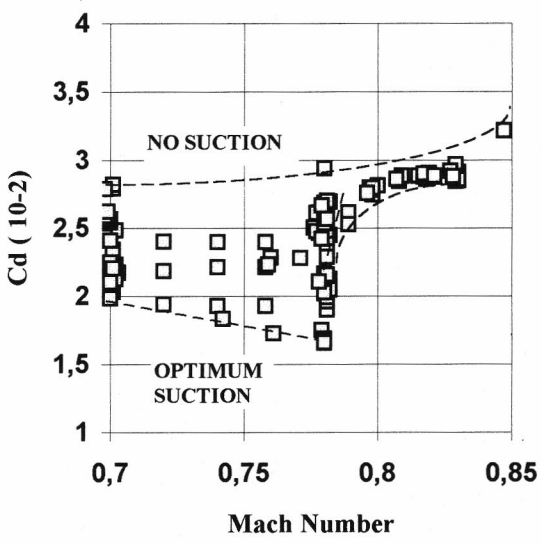

FIGURE 21 - Drag Evolution - AOA=0°
Upper Left-hand Quarter

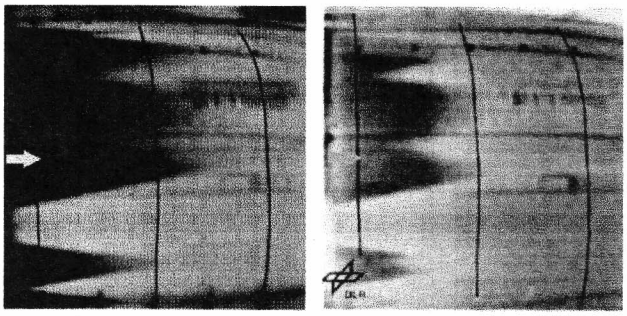

FIGURES 22a & 22b - Infrared Pictures at M=0.78 and M=0.7 - AOA=0°.

At the optimum point (M = 0.78), a 42% drag reduction was measured between tests without and with suction. Without suction, transition occurs at the beginning of the first suction chamber due to the recirculation of the air through the perforated sheet. The transition is therefore situated at about 10% of the chord. The reduction in drag obtained with our HLF nacelle compared with a fully turbulent nacelle is of the order of 50% at this operating condition.

The Mach number distributions on the surface during these tests with zero angle of attack were more severe than expected. In particular, recompression in the suction zone displayed far steeper gradients, approaching the shock limit. The cause of these differences has not yet been determined.

In order to reduce the severity of the gradients, and because it had thus far been impossible to extend the laminar flow zone beyond M = 0.78, the angle of attack was changed to 2°.

- Results at 2° angle of attack

The results obtained on the lower surface of the nacelle with an angle of attack of 2° were considerably improved. However, it was impossible to obtain a laminar flow on the upper surface, therefore all the results described below correspond to the lower part of the nacelle .

A brief analysis of the resulting performance is given in the graph showing drag as a function of Mach number in the wind tunnel (figure 23). The lower boundary indicates an extension of laminar flow up to the maximum Mach number (M = 0.845) achievable during the test, an operating condition for which the flow around the nacelle displays a strong shock behind the maximum cross-section. The maximum reduction in drag is obtained at M = 0.82 with a laminar drag equivalent to 48% of the drag without suction; the gain brought by the HLF concept compared with an entirely turbulent nacelle represents a 57% reduction in external drag.

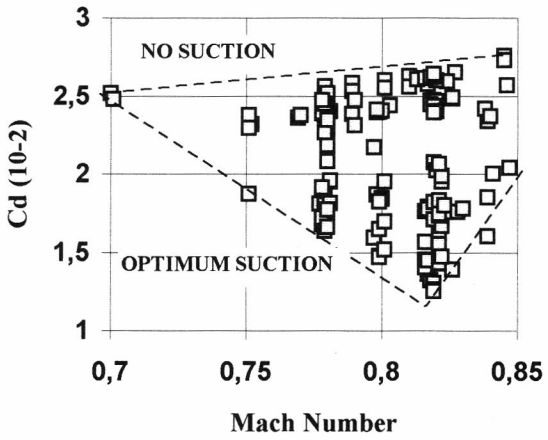

FIGURE 23 - Drag Evolution - AOA = 2°
Lower Right-hand Quarter

The extension in laminar flow associated with this reduction in drag is clearly visible in the infrared image (figure 24) which shows a laminar-to-turbulent flow transition at nearly 70% of the chord. The laminar zone covers a wide surface area limited on the upper side by the quadrant with no suction and on the lower side by a turbulent wedge whose transition originates from the holes of the static pressure taps. This result is confirmed by measurement of the hot film placed at that point, which clearly shows a virtually laminar signal, as the turbulence factor drops to $\gamma = 0.05$ (figure 25).

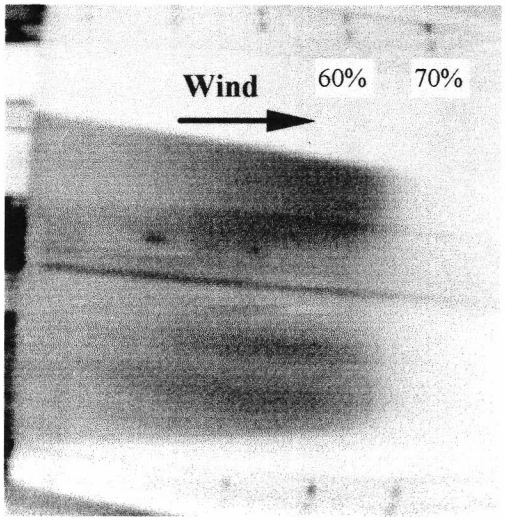

FIGURE 24 - Infra-red Picture - M=0.82^{+} - AOA=2°

The laminar zone extension obtained during tests exceeds the initial objectives (60%) and is very close to the initial predictions (70% to 73%).

FIGURE 25 - Hot film signal - M=0.82^{+} - AOA=2°

The test campaign has highlighted the effects of certain parameters on boundary layer transition. The main parameters studied were: Mach number in the wind tunnel, flow coefficient, recompression gradient in the suction range and the suction distribution.

- Influence of operating conditions

The operating conditions have a significant effect on the flow for an inlet and hence on the transition position of the boundary layer of an HLF nacelle. This has already been demonstrated with the angle of attack. The Mach number and engine flow rate are the other two important parameters. During the test campaign the Mach number in the wind tunnel varied between 0.7 and 0.845 and the massflow ratio between 0.67 and 0.79.

Figure 26a shows the change in drag with optimal suction as a function of the wind tunnel Mach number for several massflow ratios (MFR). This information can be synthesised in a different manner by plotting the change in drag as a function of the flow coefficient for different Mach numbers, as shown in figure 26b.

The graphs showing the change with external Mach number are conventional, and reveal divergence Mach numbers close to 0.83 with flow coefficients of more than 0.74, and closer to 0.78 at lower flow coefficients.

The spillage graphs are also conventional, showing drag increasing as engine massflow decreases. The variations in drag are, however, much greater than for a conventional inlet, and are associated with a loss of laminar flow and not with a shock formation. This loss of laminar flow appears when the recompression gradients in the suction zone become too high. This is shown in figure 27 which gives the drag values measured as a function of the Mach gradient in the recompression region for all the test points; this gradient is measured using two taps in this region. The figure indicates a limit value equal to 0.1.

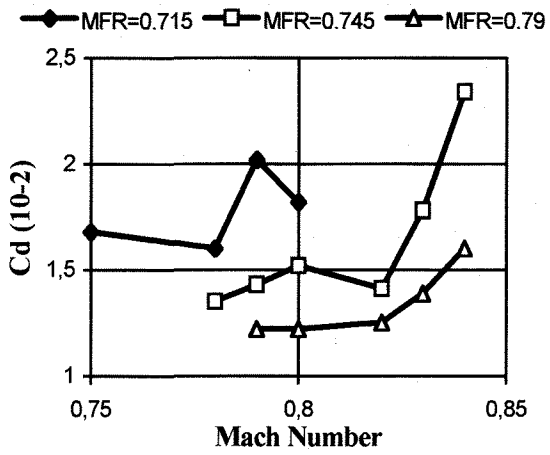

FIGURE 26a - Drag Evolution Versus Mach Number - AOA = 2°

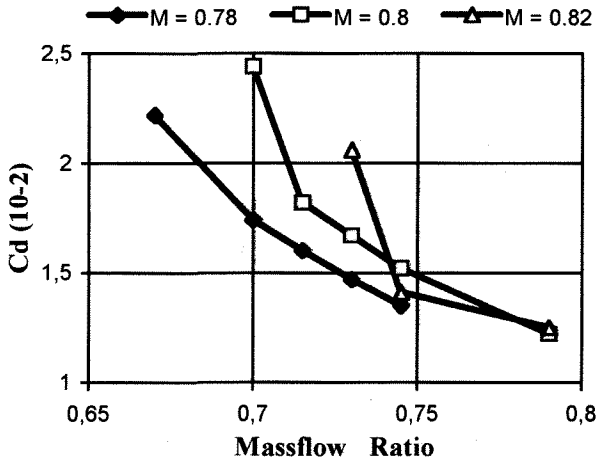

FIGURE 26b - Drag Evolution Versus Massflow Ratio - AOA = 2°

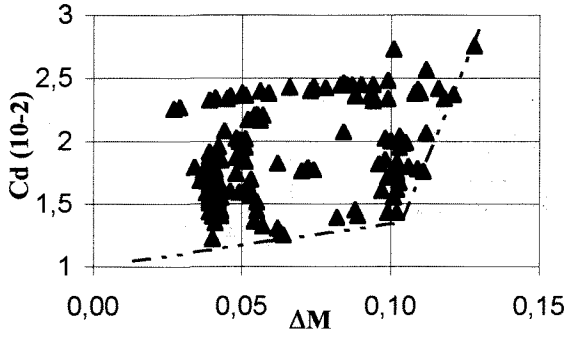

FIGURE 27b - AOA = 2° - Drag Evolution versus Recompression Intensity -

- Influence of the suction distribution

These tests helped determine the influence of the suction distribution on laminar zone extension. Excessive suction, apart from requiring a lot of power, does not improve the extension of the laminar zone; on the contrary, it can reduce it significantly.
Figure 28a associated with figures 28b and 28c shows this effect quite clearly. It shows the change in drag as a function of suction speed, which is kept at the same values in the four chambers. If the suction speed is too low, the system is ineffective and the flow will remain turbulent. At a given value, $V_{suction}$=0.11 m/s in the case presented, the flow becomes laminar over a wide range (figure 28) and drag falls to its minimum value. Beyond this, drag increases and the infrared image shows a reduced laminar flow extension. This effect will be investigated during additional analysis based on the precise surface quality measurement and on the local suction speed characterisation.

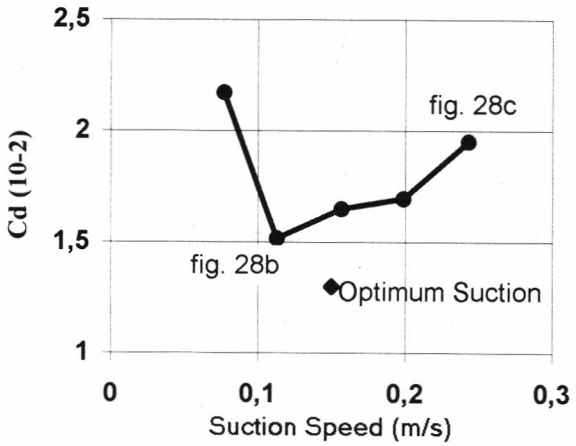

FIGURE 28a - Effect of the Suction Distribution - Mach Number = 0.8 - AOA = 2°

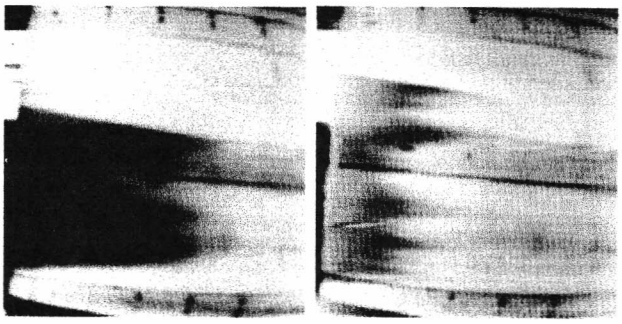

FIGURE 28b & 28c - Effect of the suction level on the Transition - Infra-red Pictures at $V_{suction}$ = 0.11 m/s and $V_{suction}$ = 0.25 m/s

Fine optimisation of the suction distribution enables the external drag to be further reduced with a slightly higher average suction speed

Conclusion regarding high-speed performance levels

The test results measured in the S1 wind tunnel at Modane did not substantiate all the computational predictions. Nevertheless, these results are highly promising, extensive laminar flow up to 70% of the chord was obtained up to the cruise flight conditions for a modern civil aircraft (M = 0.82). This laminar flow is largely conserved over a wide range of flight Mach numbers (0.7 to 0.845) and flow coefficients (0.67 to 0.79). The reduction in drag resulting from this laminar flow is just as important. Drag reductions of over 57% with respect to a fully turbulent nacelle have been measured. However, performance levels at zero angle of attack fell short of the targets and predictions, mainly due to pressure distributions different from the expected ones and insufficient quality of surface finish at the interface between the microperforated sheet and the composite material skin.

Conclusions

The laminar nacelle studies carried out by Rolls-Royce, Snecma, Hispano-Suiza, ONERA and DLR for the European programmes ELFIN II and LARA have highlighted the potential of HLF nacelles. The numerical studies carried out by partners have demonstrated the possibility of designing a hybrid laminar flow nacelle with boundary layer suction through a short-length of microporous surface. This concept makes it possible to sustain a high level of laminar flow (70% of the wetted area) throughout the cruising range, while meeting the highly stringent performance required by a modern civil aircraft under low-speed flight conditions.

The tests performed in ONERA's F1 wind tunnel fully confirmed the low-speed performance of the chosen inlet. The nacelle geometry prevents any external separation of the airflow during simulated engine failure or at idle power. The inlet delivers an airflow with pressure distortion sufficiently low for acceptance by the engine in the aircraft's flight envelope. By accepting RTO procedures, a 50 kg/s margin is available.

The high-speed tests did not confirm all the numerical predictions. Nevertheless, they clearly showed that is possible to obtain extensive laminar flow up to the cruising flight Mach number and this over a range of engine airflow. The reduction in drag resulting from laminar flow reached 57% of the drag compared with a fully turbulent nacelle. The preliminary studies showed that with this level of drag reduction, the savings in specific fuel consumption on the engine used as the basis for our study exceeded 2%.

All these results have confirmed the validity of the HLF nacelle concept and the performance gains that can be envisaged. Certain problems have been clearly highlighted, notably regarding the choice of optimum Mach number distribution and the technological design of an HLF nacelle. All these results have proved highly profitable for all the partners, to such an extent that a flying demonstrator specification is being launched with the backing of the European Community. This new programme is called HYLDA and brings together some fifteen European partners, including all those who participated in the ELFIN II and LARA programmes. It will enable the partners to design an HLF nacelle which meets industrial manufacturing and maintenance criteria, and which will subsequently undergo in-flight testing on an Airbus aircraft.

Acknowledgements

The authors would like to thank the European Community for the backing it has given these programmes. We extend special thanks to Dr Knörzer, the EC representative, for his constant encouragement throughout these studies. We would also like to thank Rolls-Royce, Snecma, Hispano-Suiza, ONERA and DLR for authorising us to publish this paper.
The ELFIN II and LARA programmes were directed by Dr Dziomba, whom we thank along with all the other partners who gave us their support and expert advice
Special thanks must go to Messrs Shipley (RR), Delaunay (Sn), Lardy and Portal (HS), Schmitt and Preist (ONERA) and Dr Rossow (DLR) for their highly efficient participation at the beginning of or throughout this programme.
The personnel at the F1 and S1 wind tunnels of the ONERA gave invaluable assistance in the low- and high-speed tests, which contributed greatly to the success of this programme. The authors thank them all for this, and in particular Messrs Raynal and Garçon. We also appreciated the extremely efficient support offered by Dr de Groot and Kreplin and Messrs Sitzmann and Baumgarten of the DLR. We are very grateful to Dr Kuhn for sharing his vast experience with us during the high-speed tests. Finally we wish to thank all the people at Hispano-Suiza, AS&T and DLR who helped manufacture and prepare the wind tunnel models.

References

(1) Laminar - The past, present and prospects AIAA'89 - R.D. Wagner and D.W. Bartlett - NASA Langley Research Center - 2nd Shear Flow Conference - March 13-16, 1989 - Tempe, AZ.
(2) 757 Testbed Boosts Laminar-flow Hopes - Flight International 26 September - 2 October 1992.
(3) HFLC for Commercial Aircraft - First ELFIN Test Results - H. Bieler, J. Preist - 1st European Forum on Laminar Flow Technology.
(4) Flight Research on Natural Laminar Flow Nacelles : A Progress Report - E.C. Hastings, J.A. Schoenster & al. - AIAA/ASME/SAE/ ASEE 22nd Joint Propulsion Conference - June 16-18, 1986 / Huntsville, Alabama.
(5) The Merits of a Hybrid Laminar Flow Nacelle - P.K. Buthiani, D.F. Keck, D.J. Lahti, E.J. Stringas - Leading Edge, General Electirc - Spring 1993.
(6) The Flight Testing of Natural and Hybrid Laminar Flow Nacelles - B. Barry, S.J. Parke, N.W. Bown, H. Riedel, M. Sitzmann - International Gas Turbine and Aeroengine Congress and Exposition - The Hague, Netherlands - June 13-16,1994.
(7) The development of a Redesign Procedure for Civil Engines Nacelles - R.V. Brooks, N.T. Birch, E.H. Kitchen - 10th ISOABE Conference - 1991.
(8) An Approximate Method of Calculating the Laminar Boundary Layer Development in Two-Dimensional, Incompressible Flow - M.R. Head - ARC R&M 3123 - 1959.
(9) Simulation Numérique de l'Ecoulement Aérodynamique autour des Nacelles - J.L. Lecordix, J.G. Fratello, J.M. Gippet - AGARD Conference Proceedings 498.
(10) Recent Progress in Inverse Methods in France P.F. Bry, O.P. Jacquotte, M.C. Le Pape - 3rd International Conference on Inverse Design

Concepts and Optimization in Engineering Sciences - Washington - 23-25 October, 1991.
(11) Laminar Instability Theory and Transition Criteria in Two and Three-Dimensional Flow - D. Arnal, M. Habiballah, E. Coustols - La Recherche Aérospatiale, N0 1984-2, 1984.
(12) Transition Prediction in Transonic Flow - D. Arnal - IUTAM Symposium Transsonicum III, Göttingen, 1988.
(13) Efficient Cell-Vertex Multigrid Scheme for the Three-Dimensional Navier-Stokes Equations - R. Radespiel, C.-C. Rossow, R.C. Swanson - AIAA Journal, Vol 28 N0 8, 1990.